Spatially resolved characterization of the turbulence in the scrape-off layer of the CASTOR tokamak

P. Devynck[1], G. Bonhomme[2], E. Martines[3], J. Stöckel[4], G. Van Oost[5], I. Voitsekhovitch[6], J. Adámek[4], A. Azeroual[6], F. Doveil[6], I. Ďuran[4], E. Gravier[2], J. Gunn[1], M. Hron[4]

[1]*Association EURATOM-CEA sur la fusion contrôlée, Saint Paul Lez Durance, France*
[2]*Université Henri Poincaré, Vandoeuvre les Nancy, France*
[3]*Consorzio RFX, Associazione EURATOM-ENEA sulla Fusione, Padova, Italy*
[4]*Institute of Plasma Physics, Association EURATOM-IPP.CR, Prague, Czech Republic*
[5]*Department of Applied Physics, Ghent University, Belgium*
[6]*Equipe Turbulence Plasma, Laboratoire PIIM, Université de Provence, Marseille, France*

Abstract

The poloidal distribution of turbulence in the scrape-off layer of the CASTOR tokamak is studied by means of a ring of 32 electric probes covering the whole perimeter of the poloidal cross section. Analysis of floating potential fluctuations in a scrape-off layer created in the top part of the machine by shifting the plasma downwards reveals a dominant periodic structure that propagates poloidally in the direction of the $E_r \times B$ drift. Its poloidal mode number is found to be equal to the local safety factor q. Correlation and pulse propagation analyses show that this high *m* mode is a signature of a single long flute-like structure that is aligned with the magnetic field and snakes around the torus several times before terminating on the limiter.

1. Introduction

Understanding the turbulence in the scrape-off layer (SOL) of tokamaks is as important as it is in the confined region. In most experimental conditions, the SOL transport is larger along the magnetic field lines except at the highest densities, as was shown in experiments in Alcator-CMod [1,2]. However, cross-field transport still plays a significant role, because it defines the radial extent over which the power and the particles are deposited on limiters, divertors and other wall components in the SOL. The thickness of the power deposition layer is one of the most important problems [3,4] facing the design of first wall components of the next step machines, which cannot handle energy flux densities greater than

~10 MW/m^2. This is particularly true with respect to ELMs, which cause sudden bursts of energy flux, not only in the parallel direction but also in the perpendicular one [5]. In order to progress in the characterization of turbulent transport processes in the SOL, and eventually find ways to control them, special diagnostics with extremely high temporal and spatial resolution are needed.

Information about the spatial features of SOL turbulence in fusion machines has been mostly obtained by Langmuir probes [see e.g. 6, 7, 8], reflectometry [see e.g. 9,10,11], or beam emission spectroscopy [12,13] but some recent results have been obtained with fast framing cameras in the visible domain [14,15]. All experiments indicate the existence of coherent structures (lifetime greater than the mean auto correlation time) with typical lifetimes between 5 and 40 μs [16-19]. The poloidal correlation lengths are all of the order of 1 cm and the turbulence is found to propagate poloidally with a velocity compatible with the local $E_r \times B$ drift. Depending on the size of the machine, these coherent events may [20] or may not [6] survive a full poloidal turn. However in most of these analyses, except in CCT [21,22] where a poloidal array covering 60° was used, the radial and poloidal extents of the probe arrays are limited to a few correlation lengths so that for example, the rotation of a structure around the poloidal section cannot be directly observed but must be deduced from poloidal velocity measurements.

In the experiment described here, we measure the poloidal structure of the turbulence using a poloidal ring of 32 electrodes uniformly distributed around the whole perimeter. The paper is organized as follows: In Section 2, we describe the special probe diagnostics that were used in the experiment. The magnetic configuration of the SOL in the CASTOR tokamak, which is essential for the interpretation of experimental data is discussed in Section 3. In section 4 the spatially resolved measurements of the SOL turbulence are presented. The results are discussed and conclusions are drawn in Section 5.

2. Probe diagnostics used in the experiment

Measurements are performed in the tokamak CASTOR [23, 24, 25]. The major radius is R=0.4 m. For this experiment a poloidal limiter of minor radius a=60 mm is used. The plasma current is varied from I_p = 5 to 10 kA. The line averaged density is $n_e = 0.5\text{-}1*10^{19}$ m^{-3}. The toroidal magnetic field is B_{tor}=1.3 T. The time evolution of the main parameters in a typical discharge is shown in Fig. 1.

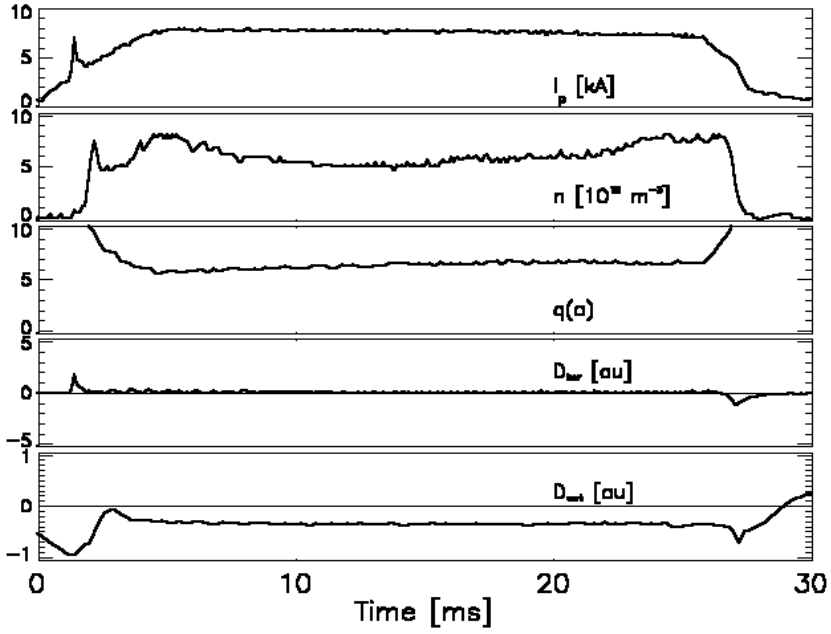

Figure 1: *Time traces illustrating a typical scenario in CASTOR. From top to bottom: Plasma Current in kA, line average density, calculated value of q at the LCFS and the horizontal (D_{hor}) and vertical (D_{vert}) position of the plasma column (in arbitrary units).*

The position of the plasma column is stabilized by the feedback system and, as seen from the corresponding traces in Fig. 1, it remains unchanged during the flat top phase of a discharge. In the SOL region, the plasma density varies in the range 0.2-0.5 10^{19} m^{-3} and the electron temperature is 8-25 eV.

The poloidal ring (see Fig. 2) consists of 32 stainless steel plates of poloidal width 10 mm and toroidal length of 70 mm, each with a 2 mm diameter graphite Langmuir probe flush-mounted at its center.

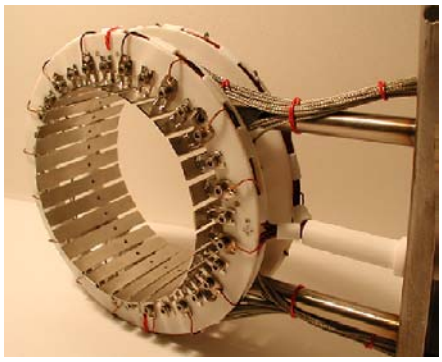

Figure 2: *Photograph of the poloidal ring. It is composed of 32 stainless steel plates distributed uniformly around the poloidal perimeter at the radius r = 58 mm. Each plate is*

equipped with a flush-mounted Langmuir probe. All the plates and probes are electrically insulated from each other allowing independent measurement and biasing.

The radius of the ring is 58 mm and its toroidal position is ϕ=140° with respect to the limiter. All the plates are electrically insulated from each other as well as from the probes inserted in them. The signals are sampled at 1 MHz and synchronized. The layout of large plates with embedded probes is motivated by the fact that the array was designed for experiments of active control of the electrostatic turbulence. However, in the present paper only passive measurements are reported. All the plates and embedded probes are kept floating in these experiments. Whether the plates or the probes are used as sensors, no significant difference is found in the main turbulent features, despite the averaging effect due to the spatial extension of the plate. As consequence, no distinction will be made hereafter. A numbering of the plates is adopted such that plate number 1 is located at the poloidal angle θ=0°, that is on the outboard midplane, and the numbering proceeds in the direction of increasing poloidal angles (towards the top, the inboard midplane and the bottom).

A rake probe, consisting of 16 tips facing the plasma, distributed radially with 2.5 mm spacing, is located at toroidal angle ϕ=180°, on top of the torus corresponding to poloidal angle θ=90°. The rake probe measures the radial profile of floating potential and its fluctuations. Its innermost tip is located at a vertical position of 50 mm relative to the center of the vessel. A single Langmuir probe is located at ϕ=320°, also on top of the torus. It is vertically positioned to be at the same radius as the poloidal ring. The correlation between signals measured by this probe and those measured by the poloidal ring, which are toroidally separated by 180°, can be calculated, giving complementary information about the orientation of the turbulent structures with respect to the magnetic field lines.

3. Magnetic configuration of the SOL

The magnetic configuration of the edge plasma on CASTOR, which is essential for correct interpretation of the fluctuation measurements, is deduced from the time-averaged floating potential measured by both probe arrays.

The typical radial profile of the time-averaged floating potential at the top of the torus as measured by the rake probe is shown in Fig 3a. The range of radii corresponding to the shadow of the poloidal limiter at the top of the torus is indicated. It is seen that the maximum of the floating potential profile appears noticeably deeper than the leading edge of the

poloidal limiter. The radial position of the maximum marks the position of the velocity shear layer (see also [24,25]), which is associated with the location of the last closed flux surface (LCFS).

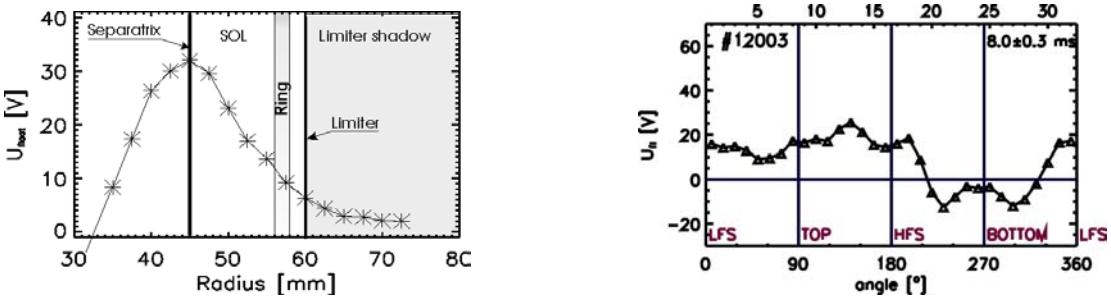

Figure 3: *a) Radial profile of the mean floating potential as measured at the top of the torus by the rake probe. The radial position of the top of the ring is marked by bars. b) Distribution of the mean floating potential around the poloidal ring.*

The time-averaged floating potential measured around the poloidal ring is shown in Fig 3b. As seen from the figure, the top half of the ring (0-180°) measures a positive floating potential (10-15 V), which is consistent with the rake probe data measured at the same radius. This means that the top of the poloidal ring is immersed in the SOL plasma. The poloidal distribution of V_{float} is rather flat in this range of poloidal angles, which indicates that the plates are located roughly on the same magnetic surface.

On the other hand, the probes on the bottom part of the ring, in particular in the range of poloidal angles 210-330°, measure the negative floating potential, which is a signature that they are effectively well inside the confined region. This is also supported by measurements of the poloidal propagation velocity of fluctuations mainly determined by the $E_r x B_t$ flow. The fluctuations at the bottom of the torus propagate poloidally in opposite directions at the bottom and at the top of the machine. This means that the top and bottom plates are on opposite sides of the shear layer, i.e. the bottom plates are in the confinement region.

All these measurements indicate that in the tokamak CASTOR, the magnetic flux surfaces are not concentric with the poloidal limiter. The respective position of the poloidal ring and the last closed magnetic flux surface is schematically depicted in Fig. 4 which shows that the magnetic axis is shifted downward by several mm.

The SOL at the top of the torus consists of two regions with different parallel connection lengths. In the shadow of the poloidal limiter, the parallel connection length is limited to one toroidal turn, $L_{//} \cong 2\pi R \cong 2.5$ m. The downshift of the plasma column creates a

secondary SOL at the top of the machine having a crescent shape in the poloidal plane and a parallel connection length of several toroidal turns. As a consequence, the same field line intersects a given poloidal section several times, with the number of intersections being related to the local safety factor. Such a magnetic configuration with a long connection length in the SOL is equivalent to that in tokamaks equipped with a toroidal limiter or a divertor.

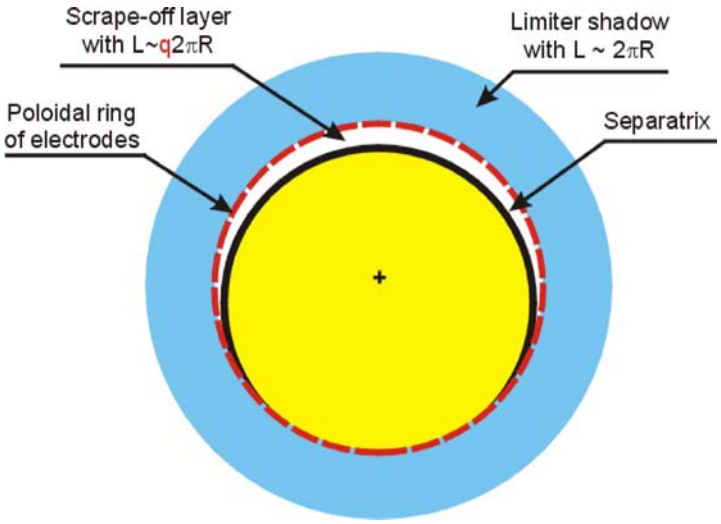

Figure 4: Respective position of the poloidal ring, limiter and the last closed flux surface (schematically*)*.

In order to prove additionally that the plates of the ring are on the same magnetic surface and therefore connected by magnetic field lines, a pulsed voltage is applied to a reference plate during the quasi-stationary phase of a discharge with edge safety factor q(a) ~ 8. The reference plate is located at the top of the poloidal ring at $\theta \sim 90^{o}$. The response to biasing is shown in Fig. 5, where an increase of the floating potential is observed on plates 32, 3, 11, 15 and 19, i.e. on every fourth plate starting from the reference plate.

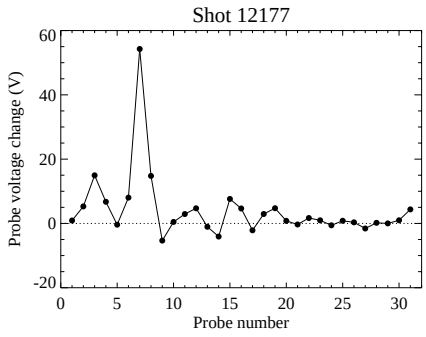

Figure 5: *Response of the probe to the voltage pulse (+180 V for 1 ms) applied to plate No. 7 located at $\theta \sim 90^{o}$ during the quasistationary phase of a discharge with edge safety factor q(a)*

~ 8 (shot 12177). The picture shows the floating potential, averaged over 0.5 ms during the biasing phase, minus the average floating potential before the pulse application.

The angular separation between these plates is consistent with the angle of the rotational transform (~45 °) for this discharge. The floating potentials of the remaining plates are unchanged. This experimental observation is interpreted as a result of the formation of a single biased flux tube, which emanates from the biased reference plate and follows the helical magnetic field lines in both directions, upstream and downstream. The biased flux tube is detected simultaneously at different poloidal angles, since it extends more than five times around the torus in this particular case. Such a response is not observed on the bottom plates that are effectively located in the confinement region.

4. Spatially resolved measurements of fluctuations in the SOL.

The spatio-temporal diagram of the floating potential fluctuations measured by the top half of the poloidal array is shown in Fig. 6a. The slow evolution, obtained by averaging over a moving window of 50 μs, has been subtracted from each signal, in order to focus on the fluctuations. Wave-like patterns propagating in the poloidal direction are clearly visible, exhibiting the presence of a dominant mode number (m = 7 in this case) and a period of 30 μs. The wave amplitude is not constant, but is modulated with a typical period of 100-150 μs. It is worth noting that the observed pattern has a similar amplitude on the low field side (θ =0°) and on the high field side (around θ = 180°), so that the fluctuations do not show a ballooning character.

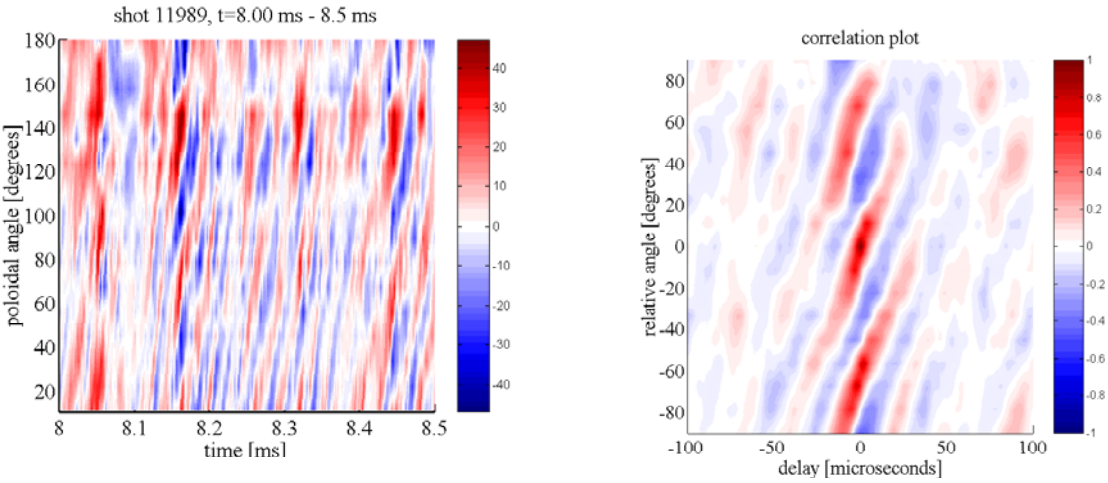

Figure 6: a) *Spatio-temporal plot of floating potential fluctuations measured by the poloidal array at the top half of the torus of the discharge.* b) *Cross-correlation of the reference probe located at the top ($\theta \sim 90^o$) with the other probes of poloidal ring located in the top half of the torus.*

The correlation between a reference probe, which is located at the top of the torus and all remaining probes of the top half of the ring is shown in Fig. 6b. It can be seen that a significant correlation is found for times of the order of 100 μs. The presence of a dominant mode (with the poloidal mode number m=7) is clearly seen from the regularity of the correlation pattern. The poloidal phase velocity of this mode is obtained from the inclination of the correlation pattern. At the top of the machine, the propagation direction is from the low to the high field side. This is consistent with the direction of the local $E_r \times B$ drift. The poloidal velocity is approximately $v_p \sim 3$ km/s in this case and is comparable to that estimated from the measured radial electric field. The radial electric field is obtained from the gradient of the floating potential profile (see Fig. 3) neglecting the contribution of the electron temperature gradient. A more precise comparison would require the measurement of the electron temperature profile which was not available during this experimental campaign. However, previous measurements indicate rather flat temperature profiles in the SOL of CASTOR [25], therefore, corrections due to temperature gradients would not be significant.

The temporal periodicity of signals measured by individual probes, which is clearly visible in Fig. 6, is a consequence of the poloidal rotation of the dominant poloidal Fourier mode. The characteristic frequency attributed to this effect is typically $f = m v_p / 2\pi a \sim 20 - 60$ kHz in CASTOR. This effect has been discussed in [26], where the conditions for the observation of a time periodicity on the correlation pattern are given.

The rake probe measurements, shown in Fig. 7a, indicate that the turbulent structures extend radially by at least 1 cm, and sometimes more. This is in agreement with previous measurements made with a 2D array of probes [20]. The radial extent of the SOL turbulence is more precisely determined by the correlation analysis of the rake probe data, which is shown in Fig. 7b. The tip used as the reference one is the one located in the proximity of the same magnetic surface than the poloidal ring.

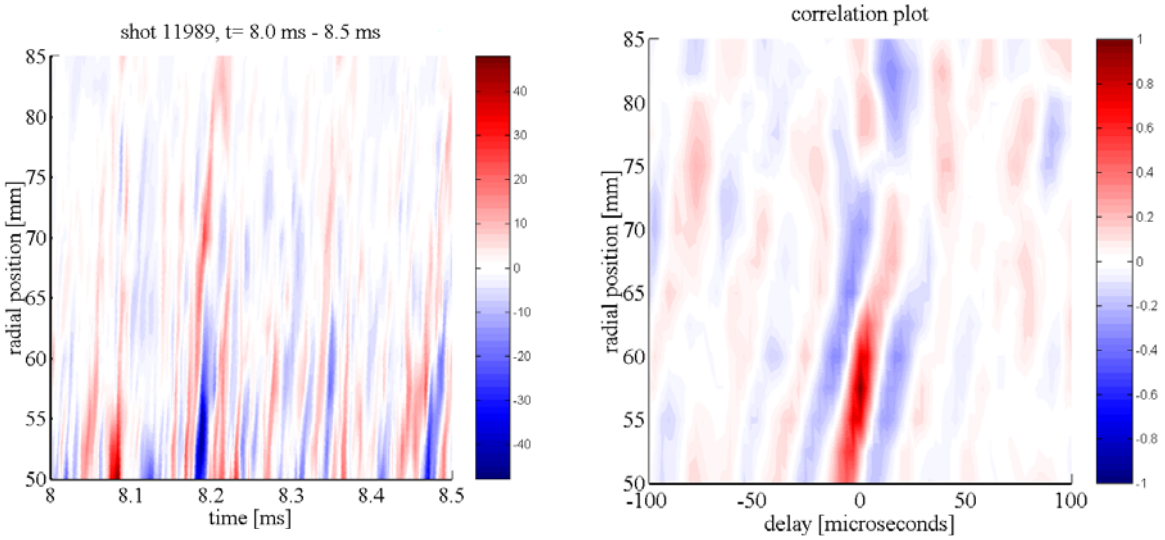

Figure 7: a) left: *Spatio-temporal plot of the floating potential fluctuations measured by the rake probe. Shot 11989, 8<t<8.5 ms. b) right*: *Cross correlation of rake probe tips with tip n°3 of the same probe as a function of lag time. Shot 11989.*

Figure 4b shows that even if the plates of the ring lie on slightly different magnetic surfaces, they register the same turbulence features.

Another interesting observation is the inclination of the patterns in the correlation plot shown in figure 7b, which might be interpreted as a signature of a propagation of turbulence in the radial direction. However, the radial velocity deduced from the inclination angle (of the order of 600 m/s) is not the result of a radial plasma motion but is rather the result of the poloidal rotation of radially elongated structures which are inclined along the poloidal direction. The reason for such inclination may be either the ExB flow gradient or the magnetic shear as discussed in ref. 6,7 and 27.

Experiments in tokamaks and stellarators show that the turbulence remains correlated over a very long distance along a given magnetic field line [6,7,9]. The correlation can remain as high as 80% even for parallel lengths of the order of 10 m and also indicates that the parallel wave number $k_{//}$ is much smaller than the perpendicular wave number $k_{\perp}$. In CASTOR the parallel correlation between the poloidal ring and a reference probe, located 180° toroidally away from the ring is studied. The reference probe is inserted in the SOL plasma from the top (the poloidal angle θ=90°) at the same radius as the poloidal ring. Figure 8 shows the correlation pattern between the reference probe and all the probes located at the

upper half of the poloidal ring. The same poloidal periodicity of the correlation pattern is observed as in Fig. 6b. This suggests that the turbulent structure associated with the reference probe crosses several times the poloidal ring. The highest correlation is observed at the plate located at θ~70°, which is the plate that is magnetically connected to the reference probe for q~7; this has been confirmed by the calculation of the magnetic field topology.

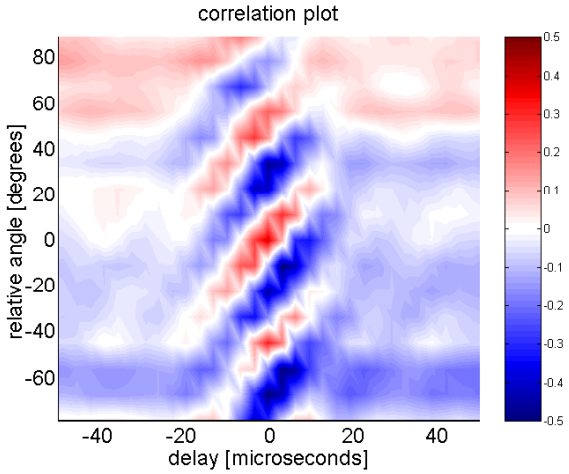

Figure 8: *Cross-correlation pattern between the reference probe and probes of the poloidal ring at the top of the torus (shot 12009). All probes measure the floating potential.*

In order to check how the high-m mode adjusts to a change of magnetic helicity in the SOL, we have performed a scan of the edge safety factor by ramping down the plasma current. The poloidal mode number spectrum has been determined by applying a sliding spatial Fourier transform on the fluctuation data of the poloidal ring. The resulting temporal evolution of the poloidal mode number spectrum is shown in Fig. 9, where the evolution of the local safety factor q is overlayed. It is clearly seen that the dominant poloidal mode number of the spectrum and the safety factor behave in the same way. This demonstrates again that the local B field helicity determines the dominant mode number of the poloidal spectrum of the turbulence in the SOL.

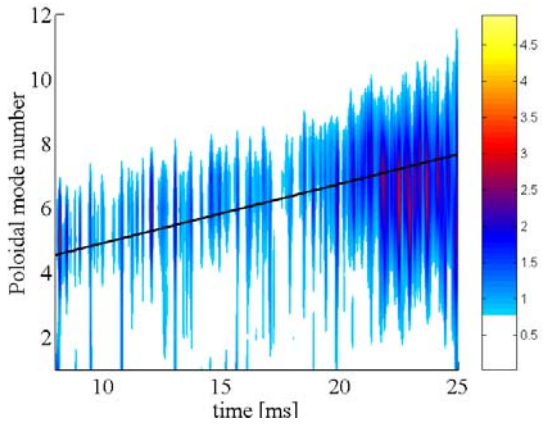

Figure 9: *Temporal evolution of the poloidal mode number spectrum during a discharge with plasma current ramp down. The amplitude of the spectrum is marked by colors. The evolution of the edge safety factor q during the discharge is marked by the black line (# 11989).*

5. Discussion and conclusions

The probe measurements have allowed to demonstrate that, in the situation with downward shifted plasma, the SOL of CASTOR is composed of two regions with different parallel connection lengths. The region close to the wall is in the shadow of the poloidal limiter and has a parallel connection length equal to one toroidal turn. A secondary SOL, created because of the plasma downshift, is observed in the upper half of the chamber. In this region the B field lines snake several times around the torus and finally terminate on the poloidal limiter. In fact, this region is similar to divertor or toroidal limiter SOL configuration. Their length is determined by the local safety factor q and by the vertical displacement Δ of the plasma column. The pulse propagation experiment reveals that the parallel connection length in the secondary SOL is at least $\sim 5 \times 2\pi R$ for the typical safety factor $q \sim 8$.

The correlation analysis of potential fluctuations, performed using as a reference either one probe of the poloidal ring or a probe located at another toroidal angle, indicates that the behaviour of the SOL turbulence is strongly linked to the configuration of the magnetic field in this region. The fluctuation measurements could be interpreted in a straightforward way assuming a single long structure aligned with the magnetic field lines, which intersects a given poloidal cross section several times, giving rise to an apparent m=q mode. This structure propagates in the poloidal direction at a velocity of the order of the local $E_r \times B$ drift. The alternating sign of the correlation pattern observed in Fig. 6b indicates a dipole character of the structure, which is also observed in other machines [27,28,16].

A possible explanation comes from the flute-like instability model in the SOL described in the refs. [29,30]. The model is based on the curvature and gradient of the magnetic field and predicts fluctuating parallel currents flowing in the SOL to the surface of the limiter. These currents charge flux tubes connected to the limiter at different potentials. In order to obtain the observed periodicity, it is necessary that only a single turbulent feature having a dipole poloidal structure exists. In that case, the helicity of the field line would reproduce the same dipole feature at different poloidal positions and would give a correlation

pattern on the ring similar to the one shown in Fig. 6. The model of Nedospasov [29] has been adopted by M. Endler et al. [6] to describe the SOL turbulence in the tokamak ASDEX where individual fluctuation events with a dipolar structure and propagating poloidally have been observed.

In our case, it has been demonstrated that the observed poloidal periodicity is due to the geometric effect described above. This effect cannot be invoked in the case of ASDEX because the spatial scale of the periodicity, geometrically created, depends on the machine size. For CASTOR a periodicity of q_a=7 at a=6.1 cm yields an equivalent wave number of k_θ=1.14 cm^{-1} which is within the expected turbulent k_θ spectrum. For a larger machine with a=1 m, for example, the same q value would give k_θ=0.07 cm^{-1} which would be outside the turbulent wave number domain and beyond the diagnostic capability as well.

The model of Nedospasov [29] requires a material surface with respect to which different magnetic flux tubes can be charged to different potentials. Hence, the configuration and size of the limiter/divertor will determine the number of flute like structures that can be excited simultaneously. In the case of CASTOR with a small poloidal limiter, only one such structure can fit into the available volume whereas several of them can be excited simultaneously in ASDEX, giving rise to a correlation pattern with several poloidal oscillations.

Acknowledgement: Authors are indebted to F. Jiranek, V. Havlik, K. Rieger, M. Satava and J. Zelenka for the design, construction of diagnostics and technical assistance in the experiment. This work has been carried out with the support of the projects No 202/03/0786 (Grant Agency of the Czech republic) and No. 2001-2056 (INTAS).

References

[1] M. V. Umansky, S. I. Krasheninnikov, B. LaBombard, and J. L. Terry , *Phys. Plasmas* **5,** 3373 (1998)

[2] B. LaBombard, M.V. Umansky_, R.L. Boivin, J.A. Goetz, J. Hughes,B. Lipschultz, D. Mossessian, C.S. Pitcher, J.L. Terry, Alcator Group, *Nucl. Fusion*, **40**, 2041-2060 (2000)

[3] G. Federici et al., *J. Nucl. Mater.*, **313-316**, 11 (2003).

[4] P. C. Stangeby, G. M. McCracken., *Nucl. Fusion* **30**, 1225 (1990).

[5] W. Fundamenski, W. Sailer and JET EFDA contributors, *Plasma Phys. Control. Fusion* **46**, 233 (2004).

[6] M. Endler, H. Niedermeyer, L. Giannone, E. Holzauer, A. Rudyj, G. Theimer, N. Tsois and the ASDEX Team, *Nucl. Fusion* **35**, 1307, (1995).

[7] J. Bleuel, M. Endler, H. Niedermeyer, M. Schubert, H. Thomsen and the W7-AS Team, *New Journal of Physics* **4**, 38 (2002).

[8] J. Petržílka, J. Stöckel, Edge Turbulence Analysis by Means of Electrical Probes on Tokamak CASTOR. *Contributions to Plasma Physics* **38** [Special Issue], 74-79 (1998).

[9] V.A. Vershkov, S.V. Soldatov, D.A. Shelukhin, V.V. Chistiakov, *Nucl. Fusion*, 39, 1783 (1999)

[10] L G Bruskin1, A Mase2, N Oyama1, K Shinohara1 and Y Miura1, *Plasma Phys. Control. Fusion* **45,** 1227–1245 (2003)

[11] T. T. Ribeiro, F. Serra, G. D. Conway, M. E. Manso, F. Ryter, L. Cupido, B. Kurzan, A. Silva, W. Suttrop, and S. Vergamota ASDEX Upgrade Team *Rev. Sci. Instrum*, **72,** 1366-1371. (2001)

[12] S.J. Zweben., D. P.Stotler, J. L. Terry, B. LaBombard, M. Greenwald, M. Muterspaugh, C. S. Pitcher, K. Hallatschek, R. J. Maqueda, B. Rogers, J. L. Lowrance, V. J. Mastrocola, and G. F. Renda Alcator C-Mod Group, *Phys. Plasmas* **9**, 1981 (2002).

[13] G. R. McKee, C. Fenzi, R. J. Fonck, and M. Jakubowski , *Rev. Sci. Instrum*, **74**,2014-2019 (2003)

[14] G. R. McKee, R. Ashley, R. Durst, R. Fonck, M. Jakubowski, K. Tritz, K.Burrell, C. Greenfield, and J. Robinson*, Rev. Sci. Instrum.* **70**, 913 (1999).

[15] J. L. Terry, S. J. Zweben, K. Hallatschek, B. LaBombard, R. J. Maqueda, B. Bai, C. J. Boswell, M. Greenwald, D. Kopon, W. M. Nevins, C. S. Pitcher, B. N. Rogers, D. P. Stotler, and X. Q. Xu *Phys. Plasmas* **10**, 1739-1747 (2003).

[16] B.K. Joseph, R. Jha, P. Kaw, S.K. Mattoo, C.V. S. Rao, Y.C.Saxena and the ADITYA Team, *Phys. Plasmas* **4**, 4292 (1997).

[17] B. A. Carreras, C. Hidalgo, E. Sanchez, M.A. Pedrosa, R. Balbin, I. Garcia Cortes, B. Van Milligen, D.E. Newman, V.E. Lynch, *Phys. Plasmas* **2**, 839 (1995).

[18] V. Pericoli-Ridolfini, A. Pietropaola, R. Cesario, F. Zonca, *Nucl. Fusion* **38**,12 (1998).

[19] R. A. Moyer, R. D. Lehmer, T.E. Evans, R.W. Conn, L. Schmitz, *Plasma Phys. Control. Fusion* **38**, 1273 (1996).

[20] E. Martines, M. Hron and J. Stöckel, *Plasma Phys. Control. Fusion* **44**, 351 (2002)

[21] G. R. Tynan, L. Schmitz, R. W. Conn, R. Doerner, R. Lehmer, *Phys. Rev. Lett*. **68**, 3032 (1992).

[22] G R Tynan, J Liberati, P Pribyl, R J Taylor and B Wells, Plasma Phys. Control. Fusion **38,** 1301–1305, (1996)

[23] J. Stockel, J. Badalec, I. Duran, M. Hron, J. Horacek, K. Jakubka, L. Kryska, J. Petrzilka, F. Zacek, M.V.P. Heller, Z.A. Brazilio, I.L. Caldas , *Plasma Phys. Control. Fusion* **41** [3A], A577-A585 (1999)

[24] G. Van Oost, J. Stöckel, M. Hron, P. Devynck, K. Dyabilin, J. Gunn, J. Horacek, E. Martines, M. Tendler, *11th Int. Toki Conference on Potential and Structure in Plasmas - Toki (Japan), 5/12/00 - 8/12/00, J. Plasma Fusion Res. SERIES,4 (2001) p. 29*

[25] G. Van Oost, J. Adámek, V. Antoni, P. Balan, J. A. Boedo, P. Devynck, I. Ďuran, J. P. Gunn, M. Hron, C. Ionita, S. Jachmich, G. S. Kirnev, E. Martines, A. Melnikov, R. Schrittwieser, C. Silva, J. Stöckel, M. Tendler, C. Varandas, M. Van Schoor, V. Vershkov, R. R. Weynants*, Plasma Phys. Control. Fusion* **45**, 621 (2003).

[26] P. Devynck, J. Stockel, J. Adamek,I. Duran,M. Hron, G. Van Oost, *Czechoslovak Journal of Physics*, vol. 53 (2003), **10**, 853**.**

[27] M Bruchhausen , R Burhenn , M Endler , G Kocsis , A Pospieszczyk , S Zoletnik and the W7-AS Team , Plasma Phys. Control. Fusion **46** (2004) 489–505

[28] M. Spolaore, V. Antoni, H. Bergsaker, R. Cavazzana, J. Drake, E. Martines, G. Regnoli, G. Serianni, E. Spada, N. Vianello, Proceedings of the 30th EPS Conference on Controled Fusion and Plasma Physics, St Petersburg, Russia, July7-11 (2003), p 2-158.

[29] A.V. Nedospasov, *Sov. J. Plasma Phys.* **15**, 659 (1989).

[30] X. Garbet , L. Laurent , J. P. Roubin ,A. Samain, *Nucl. Fusion* **31**, 967 (1991).